PUTATIVE BIOGENIC MICROTUBULES IN TERRESTRIAL IMPACT GLASS: A COMPARISON BETWEEN THE MISTASTIN AND RIES CRATERS. C. H. Ryan[1,2], G. R. Osinski[1,2], M. E. Schmidt[3], and R. L. Flemming[1,2], [1]Institute for Earth and Space Exploration and [2]Department of Earth Sciences, Western University, London, ON (email: cryan73@uwo.ca), [3]Department of Earth Sciences, Brock University, St. Catharine's, ON.

Introduction: Microscopic tubular structures with morphologies suggestive of biogenic rather than geologic origin have been extensively documented in various terrestrial glasses, including those found in ocean floor basalt [1-3] and mafic tuff [4]. Previous research by Sapers et al. [5, 6] has demonstrated the presence of these structures in impact-generated glass in the Ries impact structure of southern Germany. Impact glasses are likely to be found in all planetary impact structures [7], making them an ideal target for astrobiological investigation if biogenic microtubules are shown to be consistently found in terrestrial impact glasses.

Accordingly, I conducted a survey of several glass-rich impactite samples from the Mistastin crater in north-western Labrador, Canada, with the intent of finding and characterizing (if present) similar microtubular structures in these glasses.

Background: The Mistastin crater is a 36.4 Ma complex crater with a 28 km diameter [charcterized in e.g. 8, 9]. Its target rocks are composed of anorthosite, granodiorite, mangerite, and lesser amounts of metamorphosed gabbros and magmatic gneisses [8]. The impact melt rock composition, per [8], is heterogeneous and derived from anorthosite (~73%), with ~20% granodiorite and ~7% mangerite.

To compare, the Ries crater is a complex 24 km-diameter crater of approximately 14.8 Ma in age [10, 11]. The target was a Mesozoic sedimentary sequence overlying pre-Permian crystalline basement rocks [12]. Three distinct impactite units have been recorded: Bunte breccia, surficial "suevite", and crater-fill"suevite" [12, 13].

Both Ries and Mistastin have evidence for impact-generated hydrothermal alteration in their ejecta deposits [14], and became lacustrine basins post-impact. Hydrothermal activity especially is thought to be a crucial catalyst for promoting habitable conditions in rocks [5, 15].

Methods: Twenty glass-rich impactite thin sections from Mistastin [17] and three such samples from Ries [6] were analyzed with petrographic microscopes. As the Ries samples are already well-documented as containing biogenic tubules, the goal of investigating them was to establish a baseline for the context and morphologies expected of these tubules. Of these samples, seven were chosen for further study (six Mistastin and one Ries) (Table 1) on the basis of their containing relatively clear glass clasts with recognizable putative tubular structures.

The six Mistastin tubules were studied intensely and imaged at multiple scales, down to 100x magnification, in an attempt to compare their morphologies to those clearly defined in the Ries samples and to other, abiogenic microstructures such as devitrification or melt textures. Mistastin tubules were ranked on the basis of their subjective similarity to the Ries tubules, with comparison factors including length, diameter, degree of curvature, clustering or branching characteristics, and offset from the overall flow texture direction of the glass. The ranking scale was from 1 – 5, with 1 representing the least resemblance to Ries (and therefore lowest confidence in biogenic origin), and 5 (exclusive to Ries) representing the highest confidence level.

All seven chosen samples were then investigated by a Bruker d8 Discover micro-X-Ray Diffractometer at points-of-interest (POIs) on or near the tubules, to determine the mineral composition of crystallites within the glass.

Discussion: Despite the preponderance of tubules in Ries samples (both those studied here and in [6]) and the relative similarities in observed glass-based mineralogy between Ries and Mistastin, only two of the twenty Mistastin thin sections petrographically analyzed showed tubules that shared many characteristics with the Ries tubules. Of these, just one sample had tubules that were sufficiently similar enough in morphology to Ries to suggest a similar biogenic origin.

The resemblances between Mistastin and Ries craters are strong: both are similar in size, age, and post-depositional environment. The samples examined from both craters were polymict, glass-bearing breccias, and the glasses showed similar crystallite composition (table 1). However, there are some notable differences which may account for the apparent disparity in distribution of tubules.

The region of the Mistastin lake has undergone several periods of glaciation, resulting in estimates of 10 – 20 m to up to 100 m of post-impact differential erosion [8, 17]. This has resulted in the loss of substantial surface-level ejecta deposits; hence, the samples studied here may represent a deeper section of the crater stratigraphy [18]. Moreover, the samples collected from Mistastin are all from within the crater rim boundary [8, 17]. Ries crater, in contrast, has better-preserved ejecta deposits within and beyond the apparent crater rim, due to both post-emplacement deposition of lacustrine sediments forming a protective layer against erosion, and significantly less exposure to glacial erosion [11, 12]. This means the samples analyzed in [6] were collected from a higher stratigraphic level in the crater deposits, possibly positioning them for better exposure to favourable conditions for habitation.

Table 1. Sample descriptions, tubule descriptions, tubules rankings, and µXRD mineral estimations of the seven samples analyzed. Mistastin and Ries sample numbers and lithologies are from [17] and [6], respectively. Abbreviations used: ab (albite), and (andesine), bar (baratovite), bst (bustamite), en (enstatite), grs (grossularite), lab (labradorite), phl (phlogopite), prh (prehnite).

Sample number	Rock type	Glass description	Microtubule description	Tubule confidence ranking	µXRD minerals
MM09-046a	Suevite, polymict breccia	L. creamy beige w/ more "toasted" brown edges and medium brown short, lath-like/dendritic fracture pattern (possible devitrification tx)	POI 1A: Shadowy beige tubular feats. In l. beige glass. Straight/slightly bent lines 20 – 70 um long, 2-5 um diameter. Distributed randomly through glass, not connected to each other.	2	Lab, en, ab
MM10-007	Suevite, polymict breccia	Creamy white glass with very l. yellow-ish rim against m. – d. brown flow-tx glass. D. brown has c.gr. mx of whitish lath-like crystals.	No distinguished linear/tubular feats. Beyond lath crystals in d. brown glass.	1	lab, en, bst
MM10-009a	Polymict breccia (melt-bearing)	D. brown with streaks of gold, cont. many white-beige-gold clasts. Shows flow tx and devitrification tx.	Difficult to distinguish possible tubules from flow tx/fractures in glass.	1	ab, en
MM10-012	Polymict breccia	POI 1: Clast of l. brownish-grey glass with sketchy/shadowy tx – streak of darker material through centre of clast. POI 2: L. beige clast with m. brown mottled appearance. Some patches of lighter material assoc. w/ the brown material.	POI 1: Skinny, sinuous tubular feats. Not parallel to direction of glass flow tx. Mostly parallel to each other but some branch out from dark patch in glass. 25 – 90 um long, 2 – 5 um diameter. POI 2: Shorter, curvier tubular feats. Distributed throughout l. beige glass. Some tightly-curled tubules associated with m. brown material. 10 – 20 um long, 1 – 3 um diameter.	3	POI 1: lab, en, prh, grs POI 2: and
MM10-034c	Melt-poor polymict breccia	Golden-brown clear glass showing flow tx, some discrete variations in colour (l. to d. golden-brown, black patches). Darker speckles and streaks throughout glass.	Difficult to distinguish possible tubules from flow tx/fractures in glass. Some curved ("comma-shaped") tubules with bulbs at the end. 30 – 50 um long, 2 – 5 um diameter.	3	an, bar, phl
MM10-036	Polymict breccia	Beige glass w/ flow tx, patches of darker brown material, many partially-resorbed clasts of other minerals (incl. shocked qz).	Sinuous tubules distributed in l. beige glass. Similar to RI_10_13_5m. 20 – 80 um long, 1 – 3 um diameter (Fig. 1B).	4	An
RI_10_13_5m	Bunte breccia (polymict)	POI 1: Blob of darker beige-brown "foggy" glass within a mx of glasses ranging from transparent to d. brown. Small regions of flow tx in mx but no overarching flow pattern. POI 2: Flowing streaks of l. beige glass w/in a lighter-coloured glass.	POI 1: Distinctive tubules clustered densely at the edge of d. brown clast and dispersing throughout clast. Some are tightly-curled, others longer and sinuously curved. 15 – 75 um long, 0.5 – 3 um diameter (Fig. 1A). POI 2: Clusters of smaller, more tightly-curled tubules distributed throughout l. beige glass. 10 – 20 um long, 0.5 – 3 um diameter.	5	POI 1: and, qz POI 2: an, glass

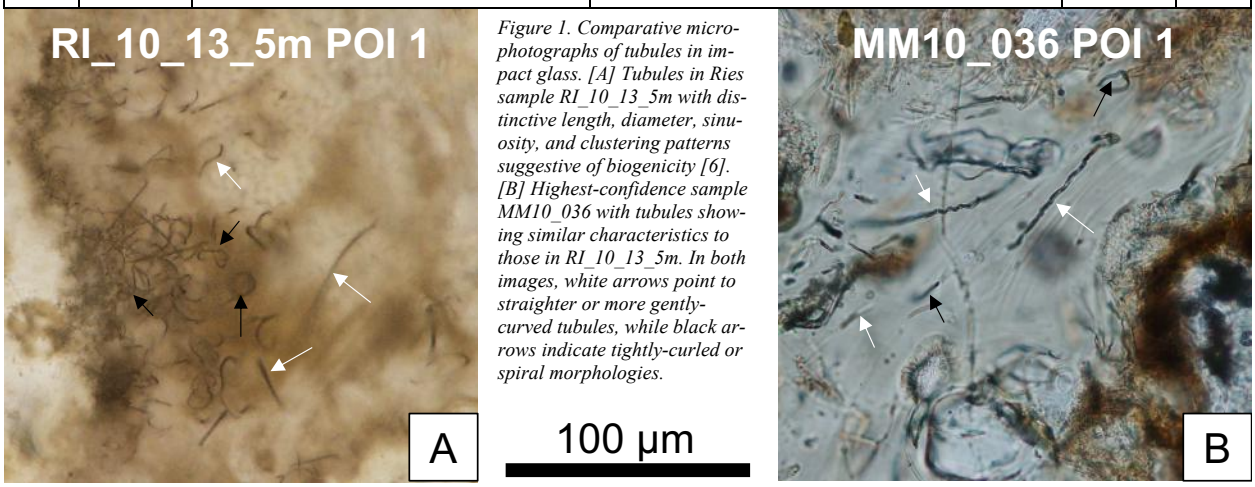

Figure 1. Comparative microphotographs of tubules in impact glass. [A] Tubules in Ries sample RI_10_13_5m with distinctive length, diameter, sinuosity, and clustering patterns suggestive of biogenicity [6]. [B] Highest-confidence sample MM10_036 with tubules showing similar characteristics to those in RI_10_13_5m. In both images, white arrows point to straighter or more gently-curved tubules, while black arrows indicate tightly-curled or spiral morphologies.

Differences in hydrothermal alteration conditions may also account for this variation. Mistastin samples analyzed in [17] show secondary mineralization of clays, zeolites, calcite, and pyrite, with the highest concentration of hydrothermal alteration products in polymict lithic breccias, such as those represented by samples MM10-036, MM10-034a, and MM10-012 (table 1). The mineralization is indicative of alteration at temperatures of <300 ºC, although no precise geothermometry measurements have been reported [17]. Hydrothermal alteration products in Ries "surface suevite" samples include montmorillonite, Ba-phillipsite, and calcite [13], evidence of lower-temperature alteration conditions (<100 – 120 ºC).

Additional study is required to both better constrain the geochemistry of the glass in Mistastin, and search for more tubules in further samples. To determine the biogenicity of the putative tubules presented here, the same analyses must be performed as in [6]. Whether biogenic tubules can be found pervasively in Mistastin rocks or not, this comparison to Ries and other craters provides valuable insights into the conditions that affect the habitability of impact glasses.

References: [1] Walton, A.W. (2008) *Geobiology 6:4*, 351-364. [2] Izawa, M.R.M. et al. (2019) *Front. Earth Sci., 7.* [3] Lepot, K. et al. (2011) *E.P.S.L., 312:1-2,* 37-47. [3] Nikitczuk, M.P.C. et al. (2016) *Geol. Soc. Am. Bull., 128:7-8,* 1270-1285. [5] Sapers, H.M. et al. (2015) *E.P.S.L., 430,* 95-104. [6] Sapers, H.M. et al. (2014) *Geology, 42:6,* 471-474. [7] Cannon, K.M. and Mustard, J.F. (2015) *Geology, 43:7.* [8] Marion, C.L. and Sylvester, P.J. (2010) *P.S.S., 58:4,* 552-573. [9] Currie, K.L. (1971) *Bull. Geol. Surv. Canada, 207,* 62. [10] Shoemaker, E.M. and Chao, E.C.T. (1961) *J.G.R., 66:10,* 3371-3378. [11] Pohl, J. et al. (1977) *Impact and Explosion Cratering,* 343-404. [12] Stöffler, D. et al. (2013) *M.A.P.S., 48:4,* 515-589. [13] Osinski, G.R. (2005) *Geofluids, 5:3,* 202-220. [14] Osinski, G.R. et al. (2013) *Icarus, 224:2,* 347-363. [15] Cockell, C.S. and Lee, P. (2002) *Biol. Rev. Camb. Philos. Soc., 77:3,* 279-310. [16] Sapers, H.M. et al. (2016) *Biosig. Pres. and Det. In Mars Analog Envs.,* #2059. [17] Mader, M.M. (2015) *Western Univ. Dissertation.*[18] Osinski, G.R. and Mader, M.M. (2018) *M.A.P.S., 53:12,* 2492-2518.